Pokrovsky-Talapov Critical Behavior and Rough-to-Rough Ridges of the Σ3 Coincidence Tilt Boundary in Mo

Boris B. Straumal,[1,2] Valery N. Semenov,[1] Olga A. Kogtenkova,[1] and Tadao Watanabe[2]

[1]*Institute of Solid State Physics, Russian Academy of Sciences, 142432 Chernogolovka, Moscow district, Russia*

[2]*Laboratory of Materials Design and Interface Engineering, Department of Machine Intelligence and Systems Engineering, Graduate School of Engineering, Tohoku University, Sendai 980-8579, Japan*

(Received 1 December 2003; published 10 May 2004)

The as-grown shape of the cylindric tilt grain boundary (GB) in Mo bicrystals grown by the floating zone method has been studied with the electron backscattering diffraction method. The seed crystals were misoriented such that the coincidence site lattice (CSL) with lowest possible inverse density of coincidence sites, a $\Sigma = 3$ was grown. The flat $(100)_{\Sigma 3CSL}$ facets were observed forming smooth edges (no slope discontinuity) with rounded rough GB portions. Rough GBs curve away from the plane of the $(100)_{\Sigma 3CSL}$ facet as x^{β} with $\beta = 1.69 \pm 0.07$ on one side and $\beta = 1.72 \pm 0.07$ on the other side. Therefore, GB roughening belongs to the Pokrovsky-Talapov universality class. Slope discontinuities between two rounded rough GB portions were also observed. This is the first experimental observation of such first-order rough-to-rough ridges predicted by the Davidson-den-Nijs model.

DOI: 10.1103/PhysRevLett.92.196101 PACS numbers: 68.35.Rh, 68.35.Ct

The phenomenon of equilibrium shape of a crystal (ECS) in contact with vacuum or vapor has been studied long [1]. Many features of the thermal evolution of free surfaces have been experimentally observed and are theoretically well understood. It is generally believed that the macroscopic equilibrium crystals are completely faceted (polyhedral) at $T = 0$. At nonzero temperature curved regions may appear in addition to the planar facets. For example, the thermal roughening of the surface facets is a realization of Kosterlitz-Thouless transition [1]. This has been observed in metallic [2], ionic [3], organic [4], and helium [5] crystals. If the flat (faceted) and rough (rounded) parts of a surface coexist, they meet at edges, which may be either sharp (slope discontinuity) or smooth (no slope discontinuity). Smooth edges between flat facets and rounded rough regions belong to the so-called Pokrovsky-Talapov (PT) universality class. Both have been observed in, e.g., lead [6–10] and helium crystals [5].

The situation becomes quite interesting if a crystal is surrounded not by vacuum or vapor, but by another crystal. From the physical point of view, the important advantage of intercrystalline boundaries (grain boundaries, GBs) in comparison with free surfaces is that the GB structure and properties depend on the interference of two crystalline lattices forming the boundary instead of one lattice forming the surface. Consider the case of two grains 1 and 2, misoriented by an angle θ_{Σ}. They form a superlattice which is common for both lattices 1 and 2 and includes the certain part $1/\Sigma$ of 1 and 2 lattice sites. Such superlattices are called coincidence site lattices (CSLs) and are characterized by the inverse density of coincidence sites Σ. In general, the symmetry of a CSL is different for different θ_{Σ} and can be noncubic even in the case of cubic lattices 1 and 2 [11,12]. However, the faceting/roughening of GBs are much less studied than those of free surfaces. The reversible faceting-roughening GB phase transition was observed initially by *in situ* heating and cooling in the transmission electron microscope at $\Sigma 11$ GB in Al near the melting temperature T_m [13]. It has been shown that faceting correlates with the so-called special structure and properties of GBs close to the coincidence misorientations θ_{Σ} [14]. GBs lose their special structure and properties (a) with increasing temperature at a critical temperature T_c and (b) with increasing deviation from coincidence misorientations $\Delta\theta = |\theta - \theta_{\Sigma}|$ at certain $\Delta\theta_c$. In [15] it has been proposed that such behavior is due to the GB roughening phase transition. However, the shape and critical behavior of GBs having both faceted and rounded rough regions have never been studied.

$\Sigma 3$ GBs have been chosen since they possess the highest possible coincidence site density. They are rather well studied and play an important role in the structure and properties of polycrystalline materials [16–24]. The section of $\Sigma 3$ CSL perpendicular to the $\langle 110 \rangle$ axis is shown in Fig. 1. The most closely packed CSL planes are shown together with respective planes for the lattices 1 and 2 forming the CSL. For example, the $(100)_{\Sigma 3CSL}$ plane is parallel to $(111)_1 // (111)_2$. It has been demonstrated that $\Sigma 3$ GBs in Cu and Ag remain faceted up to the melting temperature, T_m [20,25]. In other words, the roughening temperature, T_R, is higher than T_m for the $(100)_{\Sigma 3CSL}$ facet and the non-CSL $9R$ facet in Cu and Ag. Moreover, the facet ridges $(100)_{\Sigma 3CSL}/9R$ remain sharp up to T_m. The less closely packed $\Sigma 3$ CSL facets appear in Cu with decreasing temperature [20]. Mo has a much higher $T_m = 2896$ K and stacking fault energy $\gamma = 4.1 \times 10^{-1}$ J/m^2 [26] than Cu (respectively, $T_m = 1356$ K and $\gamma = 5.5 \times 10^{-2}$ J/m^2 [27] or 7.8×10^{-2} J/m^2 [28]). One

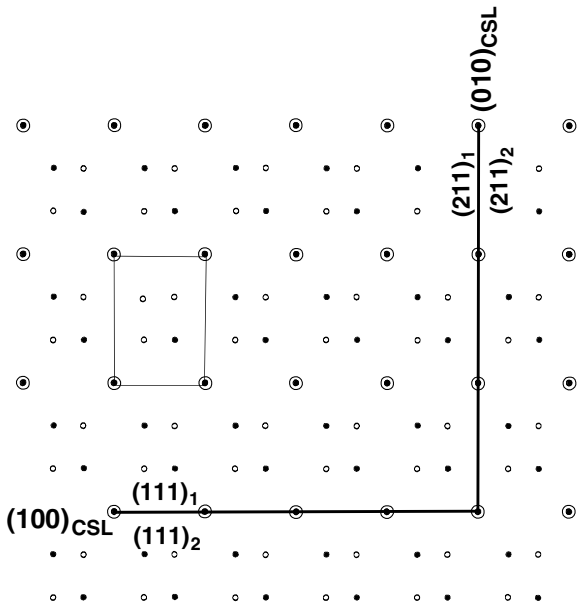

FIG. 1. Section of $\Sigma 3$ CSL perpendicular to the {110} tilt axis with CSL unit cell and positions of $(100)_{\mathrm{CSL}}$ and $(010)_{\mathrm{CSL}}$ facets.

can expect, therefore, that the $(100)_{\Sigma 3\mathrm{CSL}}$ energetic minimum in the Wulff plot is shallower in Mo than that in Cu, and $\Sigma 3$ GB in Mo would possess both flat and rough portions close to T_m. Faceting and roughening of GBs in Mo, as well as GB misorientation distribution, is technologically very important since it can govern such properties of Mo polycrystals as plasticity, brittleness, and GB sliding [29].

For the investigation of GB shape, a cylindrical Mo bicrystal having a diameter of 8 mm with two coaxial grains was grown by the floating zone technique [30,31] from Mo of 99.95 wt % purity. To stabilize the temperature distribution in the liquid zone, a circular water-cooled copper electron gun was used. The interior cylindrical grain 1 with an approximate 3 mm diameter is surrounded by the exterior ring-shaped grain 2 forming the $\Sigma 3\langle 110\rangle$tilt GB. The low growth rate of 1 mm/min ensures that the *as grown* GB is equilibrium shaped for (0.9–1.0) T_m. 2.0 mm thick platelets were cut from the grown bicrystal perpendicular to the growth axis. The GB is perpendicular to both faces of the platelet. The platelets were ground with 4000 SiC paper, polished with 3 and 1 μm diamond paste, and electrochemically polished in concentrated H_2SO_4 at voltage 20 V and current density 10 A/cm^2. The electron backscattering diffraction (EBSD) method was used to determine the individual grain orientation in the Mo bicrystal and the GB shape in the as-grown bicrystals. The EBSD method permits observation of the sample microstructure and determination of the individual grain orientation in the same experiment. The EBSD patterns were measured using a Hitachi S-4200 scanning electron microscope. The spatial resolution in the EBSD regime reaches 50 nm. Because of the large sample area, the steps between analysis points were 20 μm. We determined the individual grain orientation using the integrated software package for semiautomated fit procedure for indexing of the EBSD patterns.

The EBSD micrograph of the section of Mo bicrystal perpendicular to the common tilt axis $[110]_1/[110]_2$ is shown in Fig. 2. The brightness is proportional to the intensity of the diffracted [110] peak. The dark line where the primary electron beam meets both grains marks the GB. Two relatively short flat portions of GB can be observed between points A and B, and C and D, respectively. They are parallel both to $(111)_1$ and $(111)_2$ planes in crystallites 1 and 2. Therefore, these flat AB and CD GBs are the symmetric twin GB $(100)_{\Sigma 3\mathrm{CSL}}$. The GB portions between points A and C, and D and B are curved. To the best of our knowledge, curved $\Sigma 3$ twin GBs are observed for the first time. Previously only completely faceted twins were observed in cubic metals such as Cu, Ag, or Ni alloys and fcc Fe alloys [20,25,32,33]. The edges between flat GB facets and rounded rough regions (points A, B, C, and D) are smooth. Similar smooth edges between flat surface facets and rounded rough regions have been observed in lead [6–10] and helium crystals [5]. Near a smooth edge the shape of the curved interface varies as (see Fig. 3)

$$y = A(x - x_c)^{\beta} + \text{ higher order terms.} \qquad (1)$$

The position of edge is given by x_c. The exponent β is a critical index. The curved GB regions AE and BF have been quantified (see scheme in Fig. 3) and the respective values were calculated (Fig. 4). The $\beta_{AE} = 1.69 \pm 0.07$

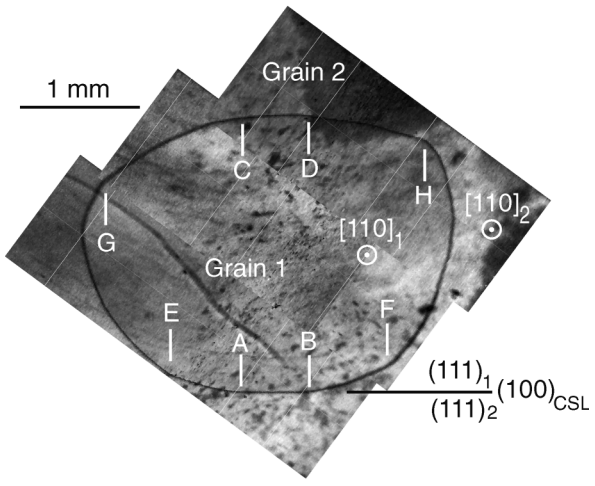

FIG. 2. EBSD micrograph of the section of Mo bicrystal perpendicular to the common tilt axis $[110]_1/[110]_2$. Flat $(100)_{\Sigma 3\mathrm{CSL}}$ facets are between points A and B, and C and D, respectively. The GB portions between points A and C, and D and B are curved. E, F, G, and H mark the slope discontinuities between two rounded rough GB portions.

FIG. 3. Scheme for the quantification of curved GB portions close to the $(100)_{\Sigma 3CSL}$ facet.

practically coincides with the $\beta_{BF} = 1.72 \pm 0.07$ value. To the best of our knowledge, these are the first critical exponents for GB roughening. There are two main models predicting β values. The mean-field approach to the problem of crystal shape neglecting the fluctuations employs a Landau-type expansion of the free energy near the roughening transition of II order [34]. It delivers $\beta = 2$, which is the signature of the square-law effective interaction between steps. The value $\beta = 2$ has never been observed experimentally. Pokrovsky and Talapov discussed the structure of a monolayer deposited on a periodic substrate incommensurate with the periodicity of the monolayer itself [35]. The steps occurring in the vicinal surface play the role of the boundaries separating individual commensurate regions in the model [35]. This theory predicts the

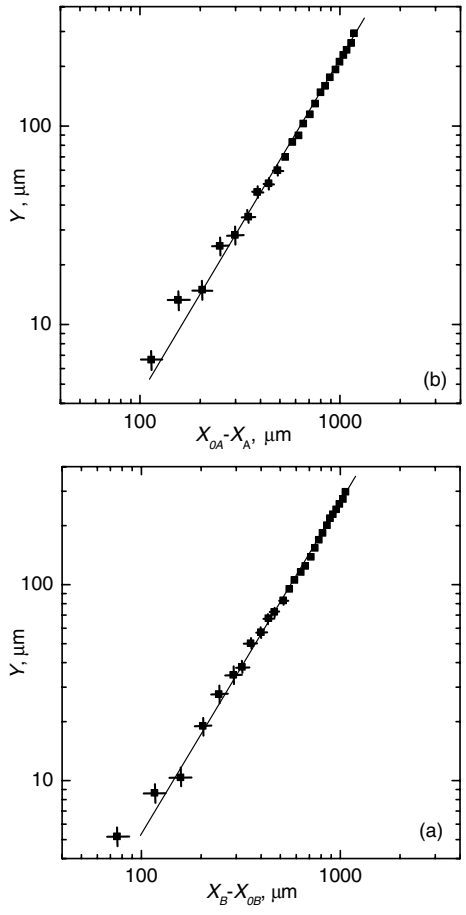

FIG. 4. Shape of the rounded GB portion close to the facet $(100)_{\Sigma 3CSL}$ in scaling coordinates. (a) between points A and E [see Fig. 2]; (b) between points B and F.

$\beta = 3/2$. Therefore, we find for the GB roughening the β values which are distinctly below the mean-field prediction and are more consistent with Pokrovsky-Talapov (PT) theory. In the recent investigation of ECS of Pb particles it has been observed that the critical exponent β measured near a (111) facet is not completely universal and varies with azimutal angle [8]. The β values distinctly fall into two groups: the first mean value is about 1.7 (similar to our value for Mo twin GB) and the second is almost equal to $3/2$. It has been shown that the β value depends on how the steps interact at the vicinal surface. Scanning tunneling microscopy demonstrates that these steps can expose either (100) or (111) microfacets. Higher exponents are connected with (100) step ledges. In our case the difference between the measured β and theoretical PT values can be due to similar GB steps.

More advanced recent ECS theories (such as the so-called body-centered solid-on-solid model on a square lattice, BCSOS) predict a rich variety of surface phenomena in addition to the traditional first and second order edges between facets and rough surface [36]. Particularly, at the edge between a facet and a rough surface a critical end point (PTE) can exist. At the one side of PTE the edge is sharp (with slope discontinuity). At the other side the edge is smooth (of PT type). PTE points have been experimentally observed in Si (113) surfaces [37]. The BCSOS model predicts also that the first-order ridge between two facets can extend into the rough region as a first-order rough-to-rough (FOR) line [36]. Another unusual possibility is the spontaneous tilted rough phase; in other words a first-order ridge forms inside the rough phase [36]. This is a rough-to-rough faceting transition with yet unknown anisotropic scaling properties. The points marked E, F, G, and H (Fig. 2) identify the rough (rounded) GB portions intersecting with slope discontinuity. This slope discontinuity cannot be explained by a triple point with a small-angle GB since the EBSD method would reveal any GB with misorientation higher than 0.5°. The symmetric position of E, F, G, and H points also supports the hypothesis of the first-order ridge inside the rough phase. In other words, such rough-to-rough ridges intersect the sample surface at points E, F, G, and H. To the best of our knowledge this is the first experimental observation of such first-order rough-to-rough ridges.

The misorientation of the studied $\Sigma 3$ GB deviates from θ_Σ. Deviation is $\Delta\theta = 3°$. This $\Delta\theta$ value is well inside of the existence area for the $\Sigma 3$ GBs, which has been reported as large as 10° to 20° for different materials [38–44]. However, the deviation $\Delta\theta$ is compensated by the intrinsic GB dislocations (IGBDs) with Burgers's vector$b_\Sigma = b\Sigma^{-0.5}$ being the lattice Burgers's vector) [45]. Each IGBD is connected with a structural GB step with a height equal to b_Σ [46,47]. GBs can also contain the dislocation-free steps. Their height is different for different CSL planes [46,47]. The presence of various

kinds of GB structural steps may explain the deviation from the exact PT value of θ and the unusual first-order rough-to-rough ridges in the GB shape.

The authors thank the Russian Foundation for Basic Research, the Deutsche Forschungsgemeinschaft, INTAS (Contract No. 03-51-3779) and NATO Linkage grant (PST.CLG.979375).

[1] C. Rottman and M. Wortis, Phys. Rep. **103**, 59 (1984).
[2] J. C. Heyraud and J. J. Métois, J. Cryst. Growth **82**, 269 (1987).
[3] T. Ohachi and I. Taniguchi, J. Cryst. Growth **65**, 84 (1983).
[4] L. A. M. J. Jetten, H. J. Human, P. Bennema, and J. P. van der Eerden, J. Cryst. Growth **68**, 503 (1984).
[5] Y. Carmi, S. G. Lipson, and E. Polturak, Phys. Rev. B **36**, 1894 (1987).
[6] C. Rottman, M. Wortis, J. C. Heyraud, and J. J. Métois, Phys. Rev. Lett. **52**, 1009 (1984).
[7] S. Surnev, K. Arenhold, P. Coenen, B. Voigtlander, H. P. Bonzel, and P. Wynblatt, J. Vac. Sci. Technol. A **16**, 1059 (1998).
[8] K. Arenhold, S. Surnev, P. Coenen, H. P. Bonzel, and P. Wynblatt, Surf. Sci. **417**, L1160 (1998).
[9] K. Arenhold, S. Surnev, H. P. Bonzel, and P. Wynblatt, Surf. Sci. **424**, 271 (1999).
[10] H. P. Bonzel, and A. Emundts, Phys. Rev. Lett. **84**, 5804 (2000).
[11] H. Grimmer, W. Bollmann, and D. T. Warrington, Acta Crystallogr. **30**, 197 (1974).
[12] H. Grimmer, Acta Crystallogr. **30**, 680 (1974).
[13] T. E. Hsieh and R. W. Balluffi, Acta Metall. **37**, 2133 (1989).
[14] B. Straumal and L. S. Shvindlerman, Acta Metall. **33**, 1735 (1985).
[15] A. N. Aleshin, S. I. Prokofiev, and L. S. Shvindlerman, Scr. Metall. **19**, 1135 (1985).
[16] F. Ernst, M. W. Finnis, D. Hofmann, T. Muschik, U. Schönberger, U. Wolf, and M. Methfessel, Phys. Rev. Lett. **69**, 620 (1992).
[17] L. M. Clarebrough and C. T. Forwood, Phys. Status Solidi (a) **60**, 51 (1980).
[18] K. Harada, S. Tsurekawa, T. Watanabe, and G. Palombo, Scr. Mater. **49**, 367 (2003).
[19] L. C. Lim and R. Raj, Acta Metall. **32**, 1177 (1984).
[20] B. B. Straumal, S. A. Polyakov, E. Bischoff, W. Gust, and E. J. Mittemeijer, Interface Sci. **9**, 287 (2001).
[21] T. Watanabe, Y. Suzuki, S. Tanii, and H. Oikawa, Philos. Mag. Lett. **62**, 9 (1990).
[22] T. Watanabe, K.-I. Arai, H. Terashima, and H. Oikawa, Solid State Phenom. **37–38**, 317 (1994).
[23] Z.-J. Wang, S. Tsurekawa, K. Ikeda, T. Sekiguchi, and T. Watanabe, Interface Sci. **7**, 197 (1999).
[24] M. Takashima, A. D. Rollett, and P. Wynblatt, Philos. Mag. A **80**, 2457 (2000).
[25] A. Barg, E. Rabkin, and W. Gust, Acta Metall. Mater. **43**, 4067 (1995).
[26] B. Pegel, Phys. Status Solidi **28**, 603 (1968).
[27] P. C. J. Gallagher, Metall. Trans. **1**, 2429 (1970).
[28] E. Murr, *Interfacial Phenomena in Metals and Alloys* (Addison Wesley, Reading, MA, 1975).
[29] S. Tsurekawa, S. Kokubun, and T. Watanabe, Mater. Sci. Forum **304-3**, 687 (1999).
[30] V. G. Glebovsky, V. V. Lomeyko, and V. N. Semenov, J. Less-Common Met. **117**, 385 (1986).
[31] V. N. Semenov, B. B. Straumal, V. G. Glebovsky, and W. Gust, J. Cryst. Growth **151**, 180 (1995).
[32] S. B. Lee, D. Y. Yoon, and M. F. Henry, Metall. Mater. Trans. A **34**, 1433 (2003).
[33] G. D. Sukhomlin and A. V. Andreeva, Phys. Status Solidi (a) **78**, 333 (1983).
[34] A. F. Andreev, Sov. Phys. JETP **53**, 1063 (1981).
[35] V. L. Pokrovsky and A. L. Talapov, Phys. Rev. Lett. **42**, 65 (1979).
[36] D. Davidson and M. den Nijs, Phys. Rev. E **59**, 5029 (2000); Phys. Rev. Lett. **84**, 326 (2000).
[37] S. Song and S. G. J. Mochrie, Phys. Rev. Lett. **73**, 995 (1994); S. SongS. G. J. MochriePhys. Rev. B**51**, 10 068 (1995).
[38] G. Dhalenne, M. Dechamps, and A. Revcolevschi, J. Am. Ceram. Soc. **65**, C11 (1982).
[39] D. J. Dingley and R. C. Pond, Acta Metall. **27**, 667 (1979).
[40] G. Hasson, C. Goux, Scr. Metall. **5**, 889 (1971).
[41] J. W. Matthews, Scr. Metall. **11**, 233 (1977).
[42] A. Otsuki and M. Mitsuno, Trans. Jpn. Inst. Met. (Suppl.) **27**, 789 (1986).
[43] T. Schober and R. W. Balluffi, Philos. Mag. A **21**, 109 (1970).
[44] T. Schober and D. H. Warrington, Phys. Status Solidi (a) **6**, 103 (1971).
[45] A. P. Sutton and R. W. Balluffi, *Interfaces in Crystalline Materials* (Clarendon Press, Oxford, 1995).
[46] A. N. Orlov, V. N. Perevesentsev, and V. V. Rybin, Sov. Phys. Solid State **17**, 1662 (1975).
[47] V. V. Rybin and V. N. Perevesentsev, Sov. Phys. Solid State **17**, 3188 (1975).